Clonal expansion capacity defines two consecutive developmental stages of long-term hematopoietic stem cells

Tatyana Grinenko,[1] Kathrin Arndt,[1] Melanie Portz,[1] Nicole Mende,[1] Marko Günther,[1] Kadriye Nehir Cosgun,[1] Dimitra Alexopoulou,[2] Naharajan Lakshmanaperumal,[3] Ian Henry,[3] Andreas Dahl,[2] and Claudia Waskow[1]

[1]Regeneration in Hematopoiesis Laboratory, Center for Regenerative Therapies Dresden; and [2]Deep Sequencing Group SFB 655, Biotechnology Center; Dresden University of Technology, 01307 Dresden, Germany
[3]Bioinformatics Service, Max Planck Institute of Molecular Cell Biology and Genetics, 01307 Dresden, Germany

Long-term hematopoietic stem cells (HSCs [LT-HSCs]) are well known to display unpredictable differences in their clonal expansion capacities after transplantation. Here, by analyzing the cellular output after transplantation of stem cells differing in surface expression levels of the Kit receptor, we show that LT-HSCs can be systematically subdivided into two subtypes with distinct reconstitution behavior. LT-HSCs expressing intermediate levels of Kit receptor (Kit^{int}) are quiescent in situ but proliferate extensively after transplantation and therefore repopulate large parts of the recipient's hematopoietic system. In contrast, metabolically active Kit^{hi} LT-HSCs display more limited expansion capacities and show reduced but robust levels of repopulation after transfer. Transplantation into secondary and tertiary recipient mice show maintenance of efficient repopulation capacities of Kit^{int} but not of Kit^{hi} LT-HSCs. Initiation of differentiation is marked by the transit from Kit^{int} to Kit^{hi} HSCs, both of which precede any other known stem cell population.

CORRESPONDENCE
Claudia Waskow:
claudia.waskow@crt-dresden.de

Abbreviations used: DEG, differentially expressed gene; HSC, hematopoietic stem cell; LT-HSC, long-term HSC; MFI, mean fluorescence intensity; MPP, multipotent progenitor; SCF, stem cell factor; ST-HSC, short-term HSC.

Hematopoietic stem cells (HSCs) replenish millions of mature hematopoietic cell types every second throughout life but also maintain the HSC pool over time. HSC function is assessed by their capacity to repopulate the blood system of lethally irradiated recipient mice in the long term. The most immature HSC pool is functionally heterogeneous, and HSCs vary in their differentiation potential and duration of reconstitution (Copley et al., 2012; Muller-Sieburg et al., 2012). However, the magnitude of repopulation, thus white blood cell output per donor HSC, was only retrospectively associated with specific reconstitution patterns determined by lineage choice (Dykstra et al., 2007). Therefore, it remains unknown whether clonal expansion capacities are predetermined in donor cells or whether the magnitude of repopulation is determined by the microenvironment of the recipient.

Kit expression is widely used for the prospective isolation of HSCs, and the stem cell factor (SCF)–Kit signaling axis is pivotal for normal pool size and function of fetal and adult HSCs (Russell, 1979; Ikuta and Weissman, 1992). Consistently, alterations in Kit signaling profoundly affect adult HSC function (Ogawa et al., 1991; Czechowicz et al., 2007; Waskow et al., 2009; Ding et al., 2012; Deshpande et al., 2013). Furthermore, *Kit* alleles resulting in hypomorphic expression of the receptor are loss of function alleles (Russell, 1979; Thorén et al., 2008; Waskow et al., 2009), suggesting that reduced densities of Kit expression correlate with loss of "stemness." In contrast, cells expressing low levels of (Doi et al., 1997; Matsuoka et al., 2011) or lacking (Ortiz et al., 1999) Kit receptor expression were suggested to contain quiescent long-term HSCs (LT-HSCs). However, differences in the clonal expansion capacities of HSCs expressing distinct levels of the Kit receptor were not reported.

The Rockefeller University Press $30.00
J. Exp. Med. 2014 Vol. 211 No. 2 209-215
www.jem.org/cgi/doi/10.1084/jem.20131115

The Journal of Experimental Medicine

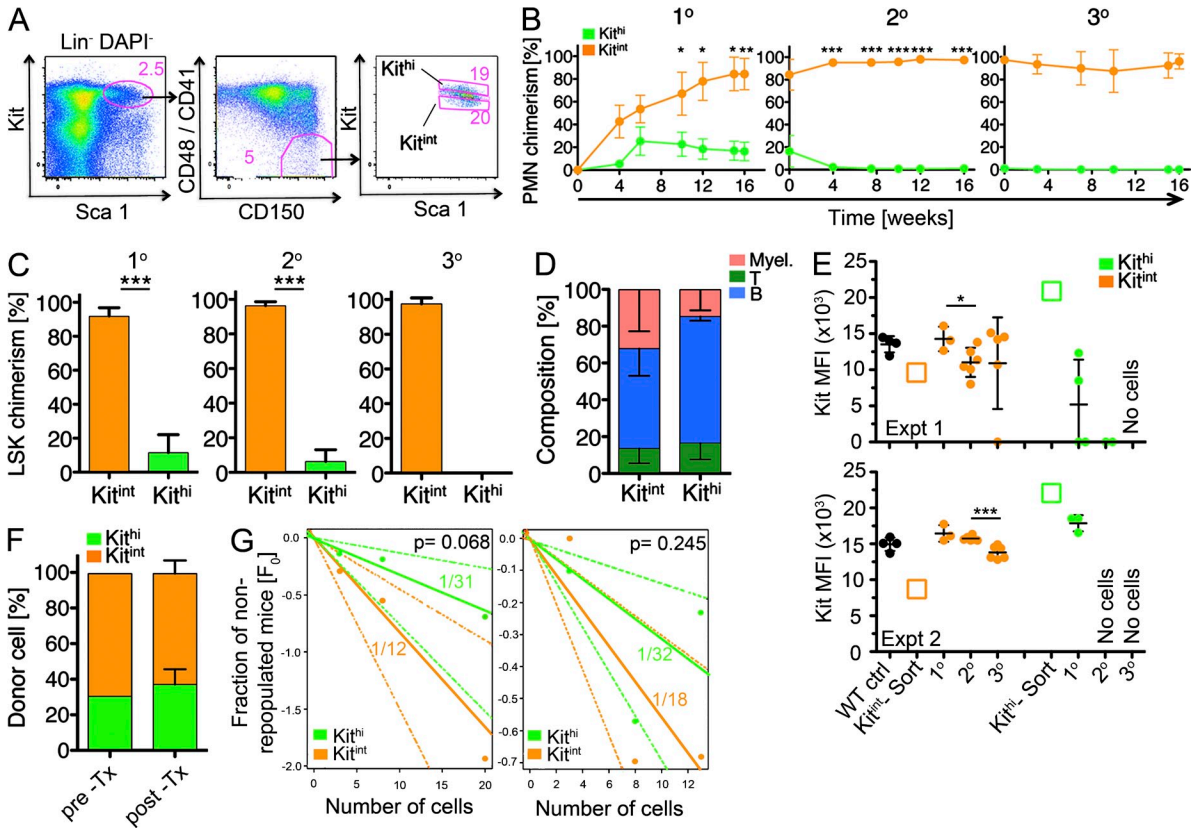

Figure 1. Prospective separation of LT-HSCs with high and low clonal expansion capacities based on the level of Kit expression. (A) BM was harvested from B6 mice, and Kit^{int} and Kit^{hi} cells within the LSK Slam population were sorted based on the indicated gates. (B–D) 50 sorted LSK Slam Kit^{int} or Kit^{hi} cells were transplanted into primary (1°), secondary (2°), and tertiary (3°) recipient mice, and donor cell contribution to the blood neutrophil compartment (B), HSC compartment (C), and donor cell composition in the blood (D) were analyzed by flow cytometry. Number of recipient mice per donor population: 1°, 3; 2°, 6; and 3°, 6. T cells (CD3$^+$), B cells (B220$^+$), and myeloid cells (Myel.; CD11b$^+$) are shown in D. $n = 3$ per condition. Mean ± SD is representative of two independent experiments. (E) BM cells from donor mice (WT ctrl), post sort cells before transplantation (open squares), and HSC progeny in recipient mice (closed circles) were isolated and analyzed for the expression density of Kit (MFI). Expt 1 (top): 50 LSK CD48$^-$ CD41$^-$ CD150$^+$ Kit^{int} or Kit^{hi} donor cells. Expt 2 (bottom): 1,000 LSK Kit^{int} or Kit^{hi} donor cells. Error bars show SD. (F) LSK Kit^{int} or LSK Kit^{hi} cells were sorted from congenic wild-type mice, mixed, and transplanted into irradiated recipients. 18 h later, contribution of Kit^{int}- or Kit^{hi}-derived cells within all donor LSK cells in the recipient's BM was determined. Mean ± SD of three recipient mice is shown. Data are representative of two independent experiments. (G) LSK Slam Kit^{int} or Kit^{hi} cells were sorted, and limited cell numbers (top: 3, 8, and 20; bottom: 3, 8, and 13) of each population were transplanted together with 3×10^5 congenic BM cells into 10 lethally irradiated recipients each. Contribution of test donor cells to neutrophils was analyzed 16 wk later. Data are from two independent experiments. *, $P < 0.05$; **, $P < 0.01$; ***, $P < 0.001$.

To assess whether expansion capacities are predetermined within donor HSCs and whether this function identifies novel cellular subtypes within the most immature HSC pool, we transplanted LT-HSCs that differed in the density of the expression of the Kit receptor. Donor cells repopulated recipient mice to two significantly different magnitudes: HSCs with intermediate levels of Kit receptor expression (Kit^{int}) contained greater expansion capacities compared with HSCs expressing high densities of the Kit receptor (Kit^{hi}), suggesting that HSC clonal growth potential is predetermined in a cell-intrinsic fashion. We further provide evidence that these HSC subtypes are two consecutive developmental stem cell stages within the most immature HSC pool and that transit from Kit^{int} to Kit^{hi} LT-HSCs marks the onset of differentiation and is associated with significant loss of expansion capacities. Gene expression profiles ex vivo and after SCF trigger suggest that the inherent differences are based on distinct cycling and adhesive activities.

RESULTS AND DISCUSSION

Prospective separation of HSCs with different expansion capacities: Intermediate levels of Kit receptor expression correlate with increased HSC potency

To assess whether distinct levels of Kit cell surface expression mark discrete types of HSCs that differ in their biological properties, we fractionated the HSC compartment into cells expressing high and intermediate densities of the Kit receptor (Fig. 1 A) and performed competitive transplantation experiments. Both donor populations engrafted stably over time (Fig. 1 B). However, Kit^{int} cells showed high repopulation of blood neutrophils and BM-resident HSCs, whereas Kit^{hi} cells contributed to sustained but low levels in both

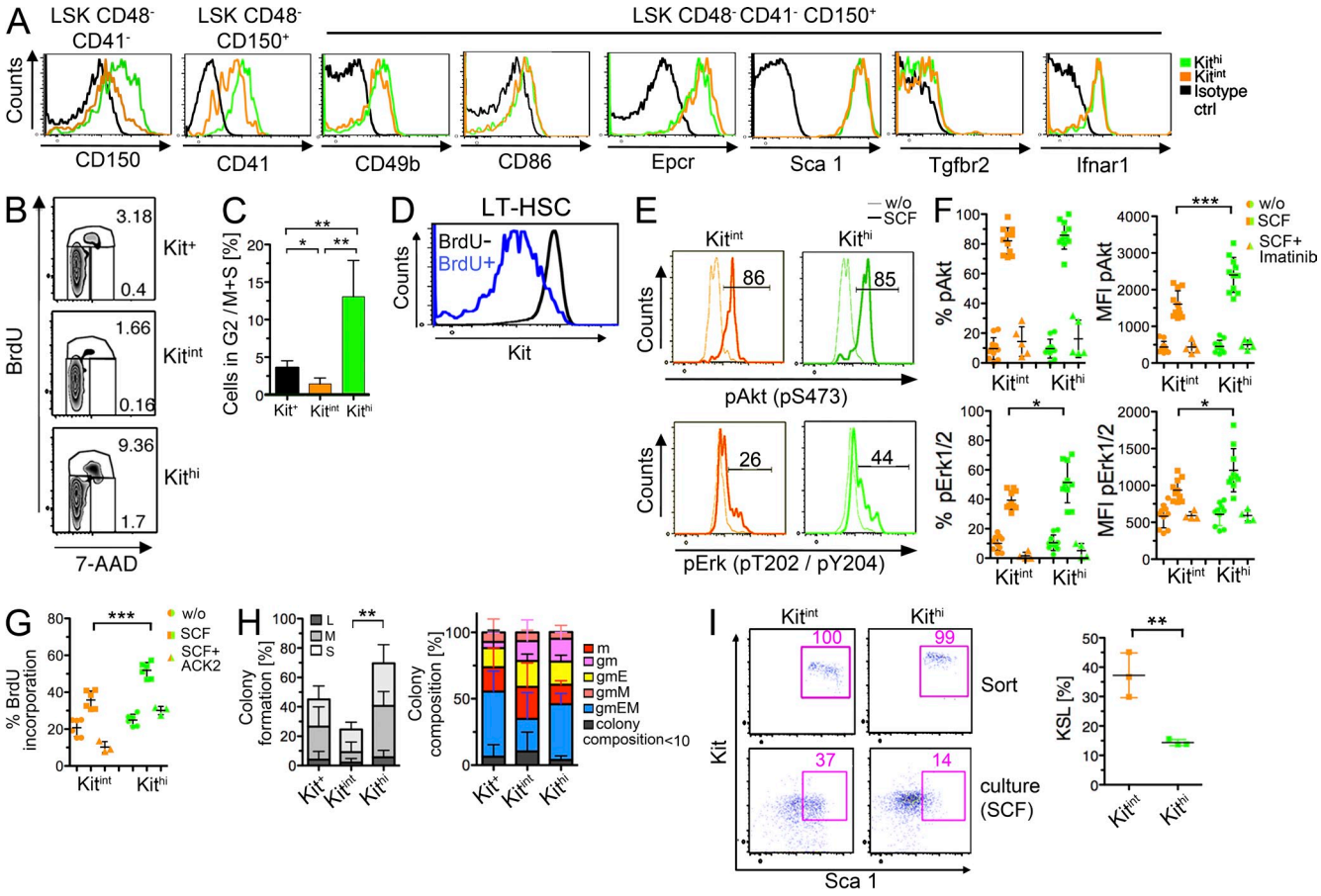

Figure 2. Density of Kit receptor expression defines two functionally distinct populations. (A) BM cells were prepared, and expression of the indicated markers was determined on Kit^{int} and Kit^{hi} cells pregated as described above the plots. Isotype control staining on LSK Slam cells is shown in black. Data are representative of two independent experiments each. (B) BrdU was injected into wild-type mice, and after 4 h, BM cells were prepared and BrdU incorporation into LS Kit^{+} cells or into LS Kit^{int} and Kit^{hi} cells was measured. (C) Plot shows summary of four mice analyzed in two independent experiments as outlined in B. (D) LSK cells were labeled with BrdU, and 330 d later, Kit expression on LS CD48^{-} CD150^{+} BrdU-positive and -negative cells was analyzed. Data are representative of two independent experiments using three mice each. (E) Lineage-depleted BM cells were cultivated with or without SCF for 15 min, and phosphorylation of Akt (top) and Erk (bottom) in LSK Slam Kit^{int} (left) or Kit^{hi} (right) HSCs was measured. (F) Plot summarizes data from three independent experiments using cells from 10 (pErk) or 11 (pAkt) mice as shown in E. For controls, four (pErk) or five (pAkt) mice were used. (G) LSK CD135^{-} Kit^{int} or Kit^{hi} HSCs were cultivated overnight in the presence or absence of SCF, BrdU was added for 4 h, and its incorporation was subsequently analyzed. Specificity was determined by using the anti-Kit inhibitory antibody ACK2 (Ogawa et al., 1991). The plot summarizes data from two independent experiments using three mice for each group. (H) Single LSK Slam CD135^{-} CD34^{-} Kit^{+}, Kit^{int}, or Kit^{hi} HSCs were cultivated in liquid culture in medium supplemented with SCF, Tpo, Il3, and Epo (left). Colony formation was analyzed after 14 d. L, large; M, medium; S, small colonies. Cell type composition of individual colonies is summarized (right). m, macrophage; g, granulocyte; E, erythroblast; M, megakaryocyte. Data shown are pooled from two independent experiments using cells from three mice each. (I) LSK CD135^{-} Kit^{int} or Kit^{hi} HSCs were cultivated as described in G, and the frequencies of Kit^{+} Sca-1^{+}–expressing cells were determined. Plot summarizes data from three mice. Changes are quantified in the plot on the right. Error bars show SD. *, $P < 0.05$; **, $P < 0.01$; ***, $P < 0.001$.

compartments (Fig. 1 C). Donor cell contribution was stable for Kit^{int} HSCs and their progeny in secondary and tertiary recipients, whereas contributions of Kit^{hi}-derived HSCs declined over time and eventually became nondetectable. There was no difference in the composition of Kit^{int}- or Kit^{hi}-derived mature white blood cells (Fig. 1 D). Expression densities of the Kit receptor on donor HSCs derived from Kit^{int} HSCs (Kit^{int}-Sort, Fig. 1 E) were increased in primary recipient mice 16 wk after transplantation and subsequently gradually declined on HSC progeny in secondary and tertiary recipient mice. In contrast, Kit expression levels on donor HSCs derived from Kit^{hi} HSCs (Kit^{hi}-Sort) were already declined in primary recipient mice, suggesting that Kit^{int} HSCs precede Kit^{hi} HSCs during differentiation.

Disparate repopulation activities after bulk transplantation can be caused by different homing activities or by varying HSC frequencies within the transplanted populations. However, homing activity between Kit^{int} and Kit^{hi} cells was undistinguishable (Fig. 1 F), and HSC frequency was also comparable as determined by limited dilution transplantations (Fig. 1 G; Hu and Smyth, 2009), suggesting that differences in repopulation activities are caused by cell-intrinsic differences in the clonal expansion capacities of donor cells. Collectively, these results indicate that clonal expansion capacities are cell-intrinsically

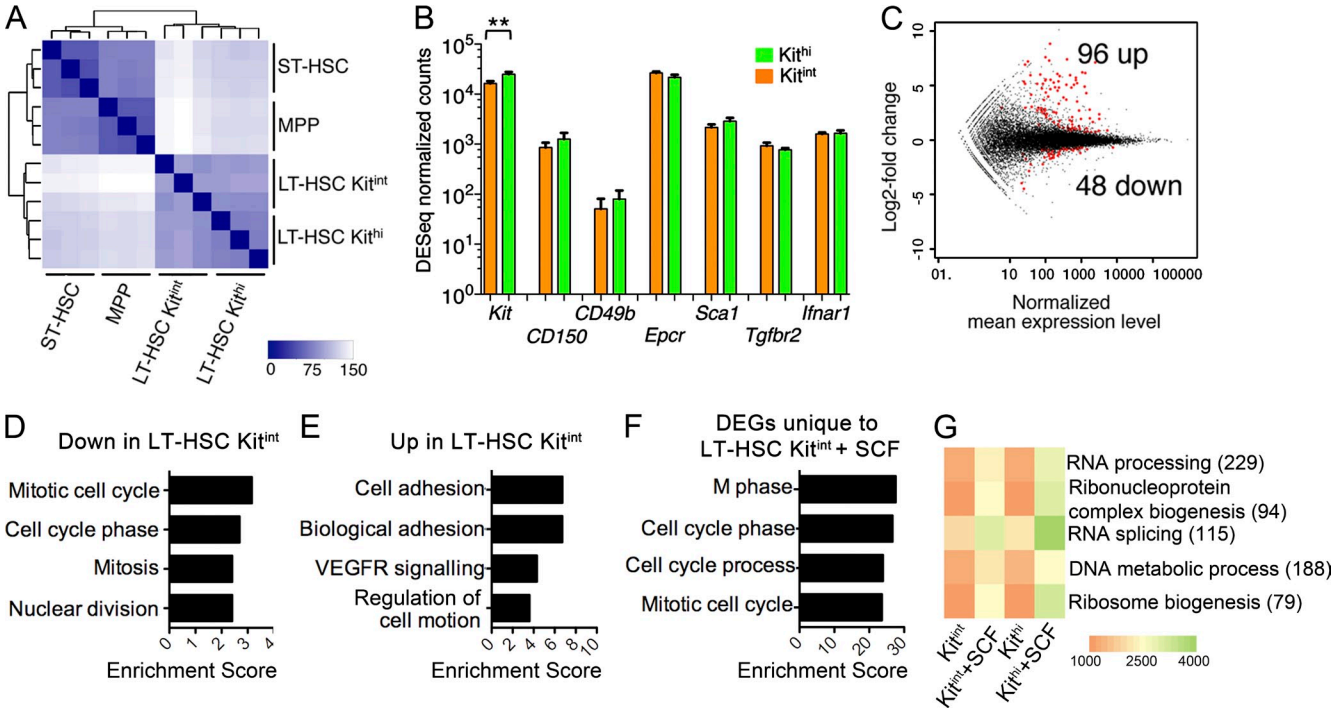

Figure 3. Kit receptor densities are indicative for HSC populations with different molecular expression programs. BM was harvested and Kit^{int} or Kit^{hi} LT-HSCs (LSK CD48$^-$ CD41$^-$ CD150$^+$ CD135$^-$ CD34$^-$), ST-HSCs (LSK CD48$^+$ CD135$^-$ CD34$^+$), and MPP cells (LSK CD48$^+$ CD135$^+$ CD34$^+$) were sorted. Whole transcriptome sequencing was performed on amplified RNA; $n = 3$ for each population. (A) Heat map of the sample to sample Euclidean distance and dendrogram showing sample to sample correlation. All biological replicates cluster well with each other, and all samples of the different populations are clearly separated from each other. (B) Graph shows DESeq-normalized counts for selected genes expressed in Kit^{int} or Kit^{hi} LT-HSCs. Protein expression from the same genes is depicted in Fig. 2 A. Mean ± SD is shown; $n = 3$; **, $P < 0.01$. (C) Comparison of gene expression profiles between Kit^{int} and Kit^{hi} LT-HSCs. Red dots represent significant DEGs at a 10% false discovery rate (FDR). (D and E) Plots show biological processes that are enriched in genes down-regulated (D) or up-regulated (E) in LT-HSC Kit^{int} cells compared with LT-HSC Kit^{hi} cells. Analysis was performed using the GO/BP database of DAVID. Enrichment scores (−log transformation of the DAVID EASE score) were calculated to determine overrepresentation of particular biological processes and are indicated on the x axis. (F) Plot shows biological processes that are uniquely enriched in genes differentially expressed in LT-HSC Kit^{int} cells after stimulation with SCF compared with LT-HSC Kit^{hi} cells after stimulation with SCF. (G) Heat map shows quantitative comparison of the expression level of genes common between DEGs of Kit^{int} ± SCF and Kit^{hi} ± SCF that are associated with the top five enriched GO biological process terms for these common genes. The number of associated DEGs is indicated in parentheses.

predetermined and that different expression densities of the Kit receptor allow for the prospective separation of two subtypes of LT-HSCs differing in that function.

Level of Kit expression marks two functionally distinct HSC populations

HSC subtypes with prolonged self-renewal activity can be found in stem cell populations that express low levels of CD49b (Benveniste et al., 2010) or high levels of CD150 (Morita et al., 2010), CD86 (Shimazu et al., 2012), and CD41 (Gekas and Graf, 2013). Furthermore, HSCs that are biased toward the development of either lymphoid or myeloid cells respond differently to stimulation with IFN-α (Essers et al., 2009) or TGF-β (Challen et al., 2010). The latter can modulate Kit cell surface expression (Sansilvestri et al., 1995). However, expression of receptors for TGF-β (*Tgfbr2*) and IFN-α (*Ifnar1*) was comparable on Kit^{int} and Kit^{hi} HSCs (Fig. 2 A). CD150 expression was inversely correlated with Kit expression, but there was no evidence for differential expression of CD49b, CD41, CD86, or other stem cell markers like Epcr (*Procr*, CD201) and Sca1 (*Ly6a*) on LSK Slam Kit^{int} or Kit^{hi} cells, suggesting lack of overlap between these populations.

Next, we showed that Kit^{int} cells were largely quiescent and in the G0/G1 phase of the cell cycle and that only Kit^{hi} cells contained actively cycling cells (Fig. 2, B and C). Consistent with this cell cycle profile, BrdU label–retaining cells were found to express low densities of the Kit receptor after a chase period of 330 d (Fig. 2 D), suggesting that Kit^{int} cells rarely cycle under steady-state conditions. We conclude that differential expression of Kit allows for the separation of active and quiescent HSCs.

Intensity of signal transduction depends on the density of Kit receptor expression

To analyze whether distinct cell biological properties may be caused by differential SCF–Kit signaling between Kit^{int} and Kit^{hi} cells, we determined the frequency and the mean fluorescence

intensity (MFI) of phosphorylated Erk and Akt after SCF trigger (Fig. 2 E). The frequency of Kit^{int} cells that phosphorylated Erk after SCF triggering was reduced compared with Kit^{hi} cells, and furthermore, the MFI of pErk and pAkt was decreased in Kit^{int} cells, suggesting that reduced densities of Kit cell surface expression result in decreased signaling activity (Fig. 2 F). Also, cell biological consequences after SCF–Kit signaling were found to be different between both populations: Kit^{int} cells proliferated to lower rates after stimulation with SCF compared with Kit^{hi} cells (Fig. 2 G), and a reduced frequency of Kit^{int} cells gave rise to colonies after 14 d of culture (Fig. 2 H). Differential signaling and proliferation depended on SCF-mediated effects because both activities were abrogated by the inhibition of Kit signaling using a pharmacological inhibitor (Fig. 2 F) or a blocking anti-Kit antibody (Fig. 2 G). Finally, reduced signaling activity in Kit^{int} cells inversely correlated with the maintenance of a Kit^{+} Sca-1^{+} stem cell surface phenotype after culture (Fig. 2 I), suggesting that high levels of Kit signaling result in differentiation but low levels of Kit signaling result in maintenance of stemness. We conclude that different densities of Kit receptor expression result in altered cell biological consequences after triggering the SCF–Kit signaling axis.

Kit^{int} and Kit^{hi} LT-HSCs are distinct molecular entities

To test for molecular differences between both HSC populations, we compared the gene expression between Kit^{int} and Kit^{hi} LT-HSCs, short-term HSCs (ST-HSCs), and multipotent progenitor (MPP) cells (Fig. 3). Unsupervised clustering revealed great homology between individual samples (Fig. 3 A), and analysis of expression counts of selected transcripts encoding for defined proteins that were previously analyzed by flow cytometry (Fig. 2 C) confirmed the purification strategy of both populations (Fig. 3 B). Comparing gene expression between Kit^{int} and Kit^{hi} HSCs revealed 96 up-regulated and 48 down-regulated genes in Kit^{int} HSCs (Fig. 3 C). The enriched functional annotation terms associated with genes differentially expressed between both populations showed an overrepresentation of terms that map to pathways related to cell cycle/division for the significantly down-regulated genes, verifying the quiescent state of HSCs that exhibit great expansion capacity after transplantation (Fig. 3 D). In contrast, we found an overrepresentation of terms related to cell adhesion pathways for the significantly up-regulated genes (Fig. 3 E), supporting the idea that retention of HSCs in their niche space instructs quiescence.

To assess whether signaling via the SCF–Kit axis results in different gene expression responses in Kit^{int} or Kit^{hi} HSCs, we compared differentially expressed genes (DEGs) between both cell types after stimulation with SCF. Consistent with the induction of cell division upon SCF trigger, DEGs that were uniquely found in Kit^{int} HSCs showed an overrepresentation of terms that map to pathways related to cell cycle (Fig. 3 F). Furthermore, DEGs common to Kit^{int} and Kit^{hi} HSCs showed a reduced expression score in Kit^{int} cells, indicating that the genes that are induced in both populations are expressed at lower levels in Kit^{int} cells (Fig. 3 G). This finding is consistent with lower levels of Kit signaling in Kit^{int} HSCs directly after trigger with SCF compared with Kit^{hi} HSCs and suggests that differential gene expression in both populations is a direct consequence of different levels of Kit signaling in situ.

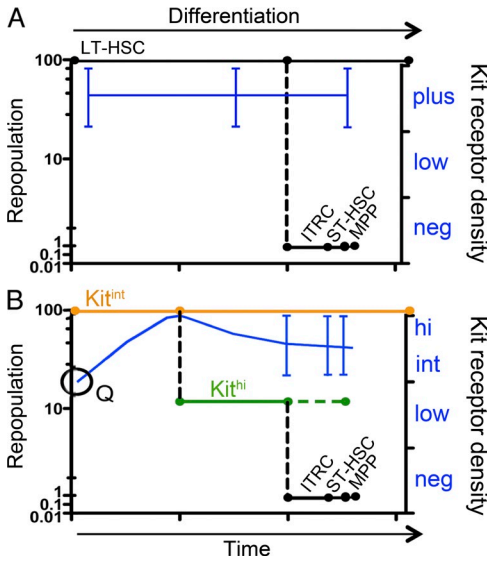

Figure 4. Present and modified model for the initiation of HSC differentiation based on transplantation experiments. (A) Present model: Kit-positive (plus) LT-HSCs repopulate recipient mice in the long term (each tick on the x axis represents ~16 wk). Kit^{+} intermediate-term reconstituting cells (ITRCs), ST-HSCs, and MPP cells repopulate recipient mice to lower levels and for much shorter time periods than LT-HSCs. The repopulation scheme of LT-HSCs, ST-HSCs, and MPP cells is based on the transplantation of 1,500 cells per population (not depicted). The repopulation scheme of ITRCs was estimated from Benveniste et al. (2010). (B) Modified model: We show that the magnitude and duration of reconstitution differs between HSC subsets and that the most immature LT-HSC compartment can be further subdivided into two novel stem cell subtypes that have inherent differences in their clonal expansion capacities. Kit^{int} HSCs repopulate recipient mice very efficiently (magnitude and duration), whereas Kit^{hi} cells can be placed between Kit^{int} LT-HSCs and ITRCs. Both magnitude and duration of reconstitution are reduced compared with Kit^{int} LT-HSCs but increased compared with ITRCs. Q, quiescent LT-HSC.

Collectively, we identified two discrete subtypes of HSCs that differ in their inherent capacities to expand and to form HSC progeny after transplantation. Kit^{int} HSCs are the most immature HSCs that may be parental to Kit^{hi} HSCs. We show that Kit expression levels negatively correlate with stemness and that reduced levels of signaling via the SCF–Kit axis are required for the maintenance of HSC function. Transition between both HSC subtypes is accompanied by a distinct loss of repopulation potential based on different clonal expansion capacities (Fig. 4). Both HSC subtypes are parental to any previously described HSC population, suggesting the identification of a novel cell type at the top of the hematopoietic hierarchy that marks initiation of differentiation. The separability of both populations will help to understand the mechanisms of self-renewal and it will be interesting to determine whether the frequency and function of both LT-HSC subsets remain constant over time during aging.

MATERIALS AND METHODS

Mice. C57BL/6 (B6) and B6.SJL-*Ptprc*^{a}*Pep3*^{b}/BoyJ (B6.SJL) mice were purchased from the Jackson Laboratory and bred and maintained under specific pathogen–free conditions in the animal facility at the Medical Theoretical Center of the University of Technology Dresden. Experiments were performed in accordance with German animal welfare legislation and were approved by the relevant authorities, the Landesdirektion Dresden.

Transplantation. For competitive transplantation, 50 lineage$^-$ Sca-1$^+$ Kit$^+$ (LSK) CD48$^-$ CD41$^-$ CD150$^+$ (Slam) Kit^{int} or Kit^{hi} cells (Fig. 1, B–E [top]) or 1,000 purified LSK Kit^{int} or Kit^{hi} cells (Fig. 1 E, bottom) were transplanted together with 5×10^5 nonfractionated BM cells into lethally irradiated (900 cGy) wild-type recipients. Test, competitor, and recipient cells carried different CD45 alleles (CD45.1$^+$, CD45.2$^+$, CD45.1$^+$ CD45.2$^+$). For serial transplantation, 5×10^6 nonseparated BM cells were injected into secondary lethally irradiated recipients. For limiting dilution analysis, 3, 8, and 20 or 3, 8, and 13 LSK Slam Kit^{int} or Kit^{hi} (CD45.1$^+$) cells were injected together with 3×10^5 nonseparated BM cells (CD45.1$^+$ CD45.2$^+$) into 10 lethally irradiated wild-type mice (CD45.2$^+$) per donor cell number. 16 wk after transplantation, donor cell chimerism was determined in blood neutrophils, and mice were scored positive when donor contribution was >1%. Frequency of the repopulating cells was calculated using ELDA software. Pairwise differences in active cell frequencies between groups were calculated as described previously (Hu and Smyth, 2009). For the first experiment, donor cells were sorted into one well and separated before transplantation, and for the second experiment, donor cells were sorted into separate wells of a 96-well plate. For homing assays, LSK Kit^{int} (CD45.1$^+$ or CD45.2$^+$) and LSK Kit^{hi} (CD45.2$^+$ or CD45.1$^+$) cells were sorted and mixed. Ratio of mixture was determined by flow cytometry, and a total of 2×10^4 cells were injected into each lethally irradiated recipient mouse (CD45.1$^+$ CD45.2$^+$). 16–18 h later, recipients were sacrificed, BM cell suspension was prepared, and donor cell ratio in LSK cells was determined.

Flow cytometry. BM cell suspensions were prepared, stained, and analyzed as described previously (Arndt et al., 2013). Antibodies (clones in parentheses) used are as follows: CD3 (2C11; 17A2), CD11b (M1/70), CD19 (1D3), CD34 (RAM34), CD45.1 (A20), CD45.2 (104), CD45R (RA3-6B2), CD86 (GL1), CD117 (2B8), CD135 (A2F10), Gr-1 (RB6-8C5), Nk1.1 (PK136), Sca1 (D7), Ter119 (Ter119), CD41 (MWReg30), Epcr (1550), CD49b (DX5), and Ifnr1 (MAR1-5A3; all eBioscience); CD48 (HM48-1) and CD150 (TC15-12F1; BioLegend); and Tgfbr2 (polyclonal; R&D Systems). MFI of Kit receptor expression was normalized between independent experiments based on the MFI of Kit expression on wild-type LS CD48$^-$ CD150$^+$ cells: (MFI Kit on donor-derived cells in experiment 1) = (MFI Kit on wild-type cells in experiment 1)/(MFI Kit on wild-type cells in experiment 2) × (MFI Kit on donor-derived cells in experiment 2).

BrdU labeling in vivo. Mice were intraperitoneally injected with a single dose of BrdU (Sigma-Aldrich; 1 mg in 200 µl PBS) and sacrificed 4 h later. Cell cycle and BrdU incorporation analyses were performed as described previously (Waskow et al., 2008). To test for label retention, mice were injected once with BrdU as described and fed BrdU-containing drinking water (1 mg/ml). BrdU-containing water was replaced every third day, and after 13 d replaced by normal drinking water. Mice were sacrificed after 330 d and BM cells were stained. A control group of three mice was sacrificed after 13 d, and 98 ± 2% of LSK cells had incorporated BrdU.

In vitro culture. To analyze phosphorylation of Akt and Erk (BD), $2–4 \times 10^6$ lineage-depleted BM cells/ml were cultivated for 15 min in DMEM supplemented with 2% FCS and 50 µM β-mercaptoethanol with or without 100 ng/ml rmSCF (R&D Systems) and with or without 100 mM Imatinib (LC Laboratories) and subsequently analyzed as described by the manufacturer. In brief, cells were fixed in prewarmed Lyse/Fix buffer (BD), washed and permeabilized using Perm Buffer III (BD), and stained for phosphorylated signaling molecules and cell surface markers for 20 min at room temperature. After a washing step, LSK Slam Kit^{int} or Kit^{hi} cells were immediately analyzed by flow cytometry. To analyze BrdU incorporation, sorted LSK CD135$^-$ Kit^{int} or Kit^{hi} cells were cultivated overnight in StemSpan medium (STEMCELL Technologies) supplemented with 100 ng/ml rmTpo, 100 ng/ml rmFlt3 ligand, 50 ng/ml rmSCF, and controls with an additional 10 µg/ml of an inhibitory anti-Kit antibody (ACK2; eBioscience). Subsequently, 10 µM BrdU was added to the cultures for 4 h, and BrdU incorporation and cell surface phenotype were analyzed. For colony growth, single LSK Slam CD34$^-$ CD135$^-$ Kit^{int}, Kit^{hi}, or Kit$^+$ cells were sorted into individual wells of a 96-well plate into StemSpan medium supplemented with 20 ng/ml rmSCF, 20 ng/ml rmTpo, 20 ng/ml rmIl3, and 5 U/ml rhEpo and cultivated for 14 d. Colony size was determined as follows: small (S) < 1 mm, medium (M) = 0.5–1 mm, and large (L) > 1.5 mm. Subsequently, cells from each colony were cytospun, and cell types were determined after May-Grünwald Giemsa staining as described previously (Arndt et al., 2013).

RNA isolation, amplification, and sequencing. For RNA isolation, LSK Slam CD135$^-$ CD34$^-$ (LT-HSC) Kit^{int} or Kit^{hi} cells, LSK CD48$^+$ CD135$^-$ CD34$^+$ (ST-HSC), and LSK CD48$^+$ CD135$^+$ CD34$^+$ (MPP) cells were sorted (FACSAria II; BD) and immediately lysed in µMACS mRNA isolation lysis buffer (Miltenyi Biotec). For SCF trigger, 7,500 sort-purified LSK CD135$^-$ Kit^{int} or Kit^{hi} cells were incubated in StemSpan medium (STEMCELL Technologies) supplemented with 50 ng/ml rmSCF for 11 h and subsequently lysed. Lysates were cleaned using LysateClear Columns (Miltenyi Biotec), and mRNA was directly isolated from the lysis buffer using SeraMag oligo(dT14) beads (Thermo Fisher Scientific). The mRNA was eluted in a volume of 5 µl of 10 mM Tris-HCL and directly subjected to subexponential RNA amplification using the WT-Ovation System (Nugen Technologies). Samples were prepared according to the manufacturer's instructions, but stopped before final Post-SPIA Modification. After bead-based purification (XP beads; Agencourt), randomly primed second strand synthesis was performed using second Strand Synthesis Module from New England Biolabs, Inc. After DNA shearing by ultrasonication (Covaris S2) and treatment with S1 nuclease (New England Biolabs, Inc.), samples were subjected to standard Illumina fragment library preparation using indexed adaptors. Resulting libraries were pooled in equimolar quantities for 75-bp single-read sequencing on Illumina HiSeq 2000 and distributed on several lanes, resulting in ∼30–90 million reads per sample.

Bioinformatic analysis. Alignment of the short reads to the mm9 transcriptome was performed with pBWA software, and a table of read counts per gene was created based on the overlap of the uniquely mapped reads with the Ensembl Genes annotation version 61 for mm9, using BEDtools (version 2.11; Quinlan and Hall, 2010). The raw read counts were then normalized with the DESeq R package (version 1.8.1; Anders and Huber, 2010), and the sample to sample Euclidean distance was computed based on the normalized counts to explore sample to sample correlation. After normalization, testing for differential expression was performed with DESeq, and accepting a maximum of 10% false discoveries (10% FDR) resulted in 96 up-regulated and 48 down-regulated genes in Kit^{int} HSCs. For SCF trigger experiments, DEGs between Kit^{int} versus Kit^{int} + SCF and Kit^{hi} versus Kit^{hi} + SCF were compared, and DEGs unique to Kit^{int} + SCF versus Kit^{int} + SCF or DEGs common to both gene lists were identified. To identify enrichment for particular biological processes associated with the DEGs, the DAVID GO/BP/FAT database (Huang et al., 2009) was used. Enrichment scores were calculated (−log transformation of the DAVID EASE score) to determine overrepresentation of particular biological processes. To quantify gene expression levels, an expression score defined as the median of all normalized counts of the DEGs associated with that particular GO term was calculated. Subsequently, expression scores for the top five GO biological process terms across the four experimental conditions were depicted in a heat map.

We thank S. Piontek and S. Böhme for expert technical assistance and V. Grinenko and B. Wielockx for discussion.

C. Waskow is supported by the Center for Regenerative Therapies Dresden, by the Deutsche Forschungsgemeinschaft (DFG) Sonderforschungsbereich (SFB) 655 (B9), SFB 127 (A3), and FOR2033 (A3), and by a grant from the European Union (FP7, CELL-PID). A. Dahl is supported by DFG SFB 655 (Deep Sequencing Group).

The authors declare no competing financial interests.

Submitted: 29 May 2013
Accepted: 6 December 2013

REFERENCES

Anders, S., and W. Huber. 2010. Differential expression analysis for sequence count data. *Genome Biol.* 11:R106. http://dx.doi.org/10.1186/gb-2010-11-10-r106

Arndt, K., T. Grinenko, N. Mende, D. Reichert, M. Portz, T. Ripich, P. Carmeliet, D. Corbeil, and C. Waskow. 2013. CD133 is a modifier of hematopoietic progenitor frequencies but is dispensable for the maintenance of mouse hematopoietic stem cells. *Proc. Natl. Acad. Sci. USA.* 110:5582–5587. http://dx.doi.org/10.1073/pnas.1215438110

Benveniste, P., C. Frelin, S. Janmohamed, M. Barbara, R. Herrington, D. Hyam, and N.N. Iscove. 2010. Intermediate-term hematopoietic stem cells with extended but time-limited reconstitution potential. *Cell Stem Cell.* 6:48–58. http://dx.doi.org/10.1016/j.stem.2009.11.014

Challen, G.A., N.C. Boles, S.M. Chambers, and M.A. Goodell. 2010. Distinct hematopoietic stem cell subtypes are differentially regulated by TGF-beta1. *Cell Stem Cell.* 6:265–278. http://dx.doi.org/10.1016/j.stem.2010.02.002

Copley, M.R., P.A. Beer, and C.J. Eaves. 2012. Hematopoietic stem cell heterogeneity takes center stage. *Cell Stem Cell.* 10:690–697. http://dx.doi.org/10.1016/j.stem.2012.05.006

Czechowicz, A., D. Kraft, I.L. Weissman, and D. Bhattacharya. 2007. Efficient transplantation via antibody-based clearance of hematopoietic stem cell niches. *Science.* 318:1296–1299. http://dx.doi.org/10.1126/science.1149726

Deshpande, S., B. Bosbach, Y. Yozgat, C.Y. Park, M.A. Moore, and P. Besmer. 2013. KIT receptor gain-of-function in hematopoiesis enhances stem cell self-renewal and promotes progenitor cell expansion. *Stem Cells.* 31:1683–1695. http://dx.doi.org/10.1002/stem.1419

Ding, L., T.L. Saunders, G. Enikolopov, and S.J. Morrison. 2012. Endothelial and perivascular cells maintain haematopoietic stem cells. *Nature.* 481:457–462. http://dx.doi.org/10.1038/nature10783

Doi, H., M. Inaba, Y. Yamamoto, S. Taketani, S.I. Mori, A. Sugihara, H. Ogata, J. Toki, H. Hisha, K. Inaba, et al. 1997. Pluripotent hemopoietic stem cells are c-kit<low. *Proc. Natl. Acad. Sci. USA.* 94:2513–2517. http://dx.doi.org/10.1073/pnas.94.6.2513

Dykstra, B., D. Kent, M. Bowie, L. McCaffrey, M. Hamilton, K. Lyons, S.J. Lee, R. Brinkman, and C. Eaves. 2007. Long-term propagation of distinct hematopoietic differentiation programs in vivo. *Cell Stem Cell.* 1:218–229. http://dx.doi.org/10.1016/j.stem.2007.05.015

Essers, M.A., S. Offner, W.E. Blanco-Bose, Z. Waibler, U. Kalinke, M.A. Duchosal, and A. Trumpp. 2009. IFNalpha activates dormant haematopoietic stem cells in vivo. *Nature.* 458:904–908. http://dx.doi.org/10.1038/nature07815

Gekas, C., and T. Graf. 2013. CD41 expression marks myeloid-biased adult hematopoietic stem cells and increases with age. *Blood.* 121:4463–4472. http://dx.doi.org/10.1182/blood-2012-09-457929

Hu, Y., and G.K. Smyth. 2009. ELDA: extreme limiting dilution analysis for comparing depleted and enriched populations in stem cell and other assays. *J. Immunol. Methods.* 347:70–78. http://dx.doi.org/10.1016/j.jim.2009.06.008

Huang, D.W., B.T. Sherman, and R.A. Lempicki. 2009. Systematic and integrative analysis of large gene lists using DAVID bioinformatics resources. *Nat. Protoc.* 4:44–57. http://dx.doi.org/10.1038/nprot.2008.211

Ikuta, K., and I.L. Weissman. 1992. Evidence that hematopoietic stem cells express mouse c-kit but do not depend on steel factor for their generation. *Proc. Natl. Acad. Sci. USA.* 89:1502–1506. http://dx.doi.org/10.1073/pnas.89.4.1502

Matsuoka, Y., Y. Sasaki, R. Nakatsuka, M. Takahashi, R. Iwaki, Y. Uemura, and Y. Sonoda. 2011. Low level of c-kit expression marks deeply quiescent murine hematopoietic stem cells. *Stem Cells.* 29:1783–1791. http://dx.doi.org/10.1002/stem.721

Morita, Y., H. Ema, and H. Nakauchi. 2010. Heterogeneity and hierarchy within the most primitive hematopoietic stem cell compartment. *J. Exp. Med.* 207:1173–1182. http://dx.doi.org/10.1084/jem.20091318

Muller-Sieburg, C.E., H.B. Sieburg, J.M. Bernitz, and G. Cattarossi. 2012. Stem cell heterogeneity: implications for aging and regenerative medicine. *Blood.* 119:3900–3907. http://dx.doi.org/10.1182/blood-2011-12-376749

Ogawa, M., Y. Matsuzaki, S. Nishikawa, S.-I. Hayashi, T. Kunisada, T. Sudo, T. Kina, H. Nakauchi, and S.-I. Nishikawa. 1991. Expression and function of *c-kit* in hemopoietic progenitor cells. *J. Exp. Med.* 174:63–71. http://dx.doi.org/10.1084/jem.174.1.63

Ortiz, M., J.W. Wine, N. Lohrey, F.W. Ruscetti, S.E. Spence, and J.R. Keller. 1999. Functional characterization of a novel hematopoietic stem cell and its place in the c-Kit maturation pathway in bone marrow cell development. *Immunity.* 10:173–182. http://dx.doi.org/10.1016/S1074-7613(00)80018-7

Quinlan, A.R., and I.M. Hall. 2010. BEDTools: a flexible suite of utilities for comparing genomic features. *Bioinformatics.* 26:841–842. http://dx.doi.org/10.1093/bioinformatics/btq033

Russell, E.S. 1979. Hereditary anemias of the mouse: a review for geneticists. *Adv. Genet.* 20:357–459. http://dx.doi.org/10.1016/S0065-2660(08)60549-0

Sansilvestri, P., A.A. Cardoso, P. Batard, B. Panterne, A. Hatzfeld, B. Lim, J.P. Lévesque, M.N. Monier, and J. Hatzfeld. 1995. Early CD34high cells can be separated into KIThigh cells in which transforming growth factor-beta (TGF-beta) downmodulates c-kit and KITlow cells in which anti-TGF-beta upmodulates c-kit. *Blood.* 86:1729–1735.

Shimazu, T., R. Iida, Q. Zhang, R.S. Welner, K.L. Medina, J. Alberola-Lla, and P.W. Kincade. 2012. CD86 is expressed on murine hematopoietic stem cells and denotes lymphopoietic potential. *Blood.* 119:4889–4897. http://dx.doi.org/10.1182/blood-2011-10-388736

Thorén, L.A., K. Liuba, D. Bryder, J.M. Nygren, C.T. Jensen, H. Qian, J. Antonchuk, and S.E. Jacobsen. 2008. Kit regulates maintenance of quiescent hematopoietic stem cells. *J. Immunol.* 180:2045–2053.

Waskow, C., K. Liu, G. Darrasse-Jèze, P. Guermonprez, F. Ginhoux, M. Merad, T. Shengelia, K. Yao, and M. Nussenzweig. 2008. The receptor tyrosine kinase Flt3 is required for dendritic cell development in peripheral lymphoid tissues. *Nat. Immunol.* 9:676–683. http://dx.doi.org/10.1038/ni.1615

Waskow, C., V. Madan, S. Bartels, C. Costa, R. Blasig, and H.R. Rodewald. 2009. Hematopoietic stem cell transplantation without irradiation. *Nat. Methods.* 6:267–269. http://dx.doi.org/10.1038/nmeth.1309